Experimental Thermal and Fluid Science 117 (2020) 110149

Contents lists available at ScienceDirect

Experimental Thermal and Fluid Science

journal homepage: www.elsevier.com/locate/etfs

Experimental study on estimation of diversion rate in porous bottom intakes for non-sediment flow

Salman Pouresmaeil[a], Mahmoud F. Maghrebi[b,c,*]

[a] Civil Eng. Department, Faculty of Engineering, University of Bojnord, Iran
[b] Civil Eng. Department, Ferdowsi University of Mashhad, Iran
[c] Civil Eng. Department, Faculty of Engineering, Ferdowsi University of Mashhad, Iran

ARTICLE INFO

Keywords:
Spatially varied flow
Porous bottom intake
Dimensional analysis
Discharge coefficient

ABSTRACT

To divert water from rivers, several structures can be employed. Bottom intake is one of the hydraulic structures which is generally used for this purpose in steep streams. Bottom racks are associated with the problems such as deformation, corrosion, vibration and clogging by foliage, sediments, and freezing. A new type of bottom intakes is introduced to overcome these difficulties in which the racks are replaced by a trench filled with a coarse porous medium. In the present study, we analyze the experimental results of a systematic series of measurements conducted in a two-storey laboratory flume. Measuring the diverted discharge is done alongside other important factors such as grain size distributions, total and remained discharges, velocity, and intake geometric properties. Furthermore, the results of our experiments are compared with those obtained from the formulas proposed in previous studies. The hydraulic characteristics of these formulas are investigated, and the necessary points for their improvement are determined. Also, we introduce new formulas for estimating discharge coefficient and diversion rate based on dimensional analysis, our experimental data, and multivariate regression. The validation of these formulas is verified through the hydraulic principles describing intake behaviors and statistical verification tests. Comparison between the calculated data and our measurements shows that the proposed formulas are in good agreement with the experimental results.

1. Introduction

Many types of water intakes are classified for diverting water from a river. Bottom intakes are generally used in small mountainous rivers where steep slopes, rapid flooding, severe sediment transport, and irregular bed configuration prevent the use of other diverting structures [1]. Bottom intakes are also used in small hydropower plants [2,3]. They are the best choices for rivers with a longitudinal gradient greater than 1% [4,5].

In general, a trash rack is designed on the surface of bottom intakes to prevent sediments from passing through the channels. This type of bottom intake is known as the bottom rack or the Tyrolean intake [6,7]. The problems such as corrosion of bars, freezing, clogging, and sediment transition to the water distribution system restrict the applicability of this type of intake [8,9]. Bottom racks are extensively used, particularly in small hydropower plants; thus, numerous researchers have worked on improving the inclination and shape of trash racks to reduce the aforementioned problems [10–14]. Nevertheless, sediment accumulation in water distribution systems and clogging of intakes remain as the most important problems of bottom racks (Table 1) [15,16].

Using porous media for drainage is one of the natural methods to remove sediment and other contaminants of water [17]. In 2009, a new type of bottom intake was introduced in which trash racks are replaced by a porous medium [18]. In this type of intakes, water drains through a porous medium, which has an arbitrary granular size. Then water is conducted to the main channel via the diversion conduit (Fig. 1). We call this type of intakes as "porous bottom" in order to distinguish it from bottom racks.

In general, 11 profiles can be assumed for the flow profile in the main channel, as shown in Fig. 2. It depends on the slopes of the channel before and after the intake as it is affected by the slope and diversion rate of the intake. In this figure, the CDL line shows the critical depth and the NDL indicates the normal depth. BW also shows the backwater curve (increasing depth along the intake) and DD indicates the drawdown curve (decreasing depth along the intake). However, in the experiments performed for this study, profiles (g) and (h) were observed.

* Corresponding author.
E-mail address: maghrebi@um.ac.ir (M.F. Maghrebi).

https://doi.org/10.1016/j.expthermflusci.2020.110149
Received 24 August 2019; Received in revised form 10 April 2020; Accepted 16 April 2020
Available online 20 April 2020

Table 1
Classification of encountered problems in 50 small hydro-power plants that use the bottom rack in Norway (16).

Types of problems	Number of intakes	Categories of problems
Branches, Leaves, Twigs, Turf	19	Floating debris
Other problems	2	
Air entrainment, Vortex formation	4 + (1)*	Air
Air in pipe	(1)*	
Sediments in the intake pond	10 + (1)*	Sediment
Wear on the turbine	2	
Frazil ice blocking the entrance to the reservoir	4	Ice
Frazil ice blocking the trash rack	3	
Ice formation in the penstock	3	
Breaking-up of ice blocking the trash rack	1	
Breaking-up of ice leading to damage	1	
Ice problem in the spillway area	1	
Freezing of the gate	1	
Other problems or unspecified	4	
Environmental	0	None

* The numbers in brackets represent power plants where the problems have been solved.

It is clear that the diversion of any specified amount of water through the porous bottom requires a larger structure than the bottom rack. In addition, the efficiency of the porous bottom is reduced via sediment deposition and hydraulic conductivity reduction [19]. Although a larger structure has to be constructed, the benefits of porous bottom in comparison with the bottom rack are the lower cost of construction and maintenance, higher compatibility with river morphology, reduction of clogging and ice problems, and elimination of sediments in outflows [19,20].

In previous researches, several formulas were proposed for estimation of the diverted discharge in porous bottom based on experimental data. There are several inconsistency issues between the expected performance of the porous bottom and these formulas. We think that these incompatibilities are due to the limitation of parameters studied in previous experiments. As a result, the validity of these formulas is limited to a relatively short range of parameter variations. Therefore, to achieve a more precise formulation, more parameters should be considered than those in previous works. In addition, this study is limited to supercritical flow because bottom intakes are normally used in the mountainous rivers with steep slopes. The Froude number of the experiments are varied from 1.1 to 2.0 for the total discharge in the upstream and 1.1 to 2.6 for remaining flow.

Motivated by the above discussion, our research focuses on the hydraulic behavior of porous bottoms in non-sediment flow. To reach this goal, we first use dimensional analysis to identify the most important parameters that have an impact on the flow. Then our experiments are designed based on dimensional analysis and a new experimental setup is built.

One of the main contributions of this study is to propose a new formulation for estimating discharge by applying multivariate regression to the experimental observations. Also, we assume that water flow on the top surface of porous bottoms is similar to that of orifices; however, in previous studies, the flow was analyzed through the Bernoulli equation with simplified assumptions. We take a lot of data in more than 400 series of experiment to produce our new model.

The rest of this paper is structured as follows. In Section 2, we briefly review previous researches and focus on the evidence that shows the incompatibility of the proposed formulas with theoretical foundations. In the next section, the basis and methodology of the present research are explained, which includes dimensional analysis and describes the experimental setup. Then the results of the experiments are reported and the corresponding mathematical model is extracted. Finally, the findings of this study are summarized and concluded.

2. Literature review

One of the first hydraulic descriptions of bottom intakes was provided by Garot in 1939 [21]. De Marchi [22], Bouvard [23], Orth et al. [24], and others followed this line of research, with investigations continuing up to recent years [2,25–27]. However, despite extensive research on bottom racks, investigation on porous bottoms remains limited. We assume that the flow field above a porous bottom is one-dimensional and has a gradually varied flow because of the similarities between the flow diversion of a porous bottom and a bottom rack. Therefore, pressure distribution remains hydrostatic at each cross-section of the flow. It is worth mentioning that the flow field is characterized by a departure from the hydrostatic pressure distribution in practice; because the streamlines have curvature, particularly when the top surface of the intake is inclined [28]. Based on these assumptions, the dynamic equation for a steady spatially varied flow in a prismatic channel may be written as [29]

$$\frac{dy}{dx} = \frac{S_0 - S_f - \left(\frac{\alpha Q}{gA^2}\right)\left(\frac{dQ}{dx}\right)}{1 - Fr^2}, \tag{1}$$

where y is the flow depth, x is the longitudinal intake axis, S_0 is the bed slope, S_f is the friction slope, α is the energy coefficient, Q is the flow discharge, g is the gravity acceleration, A is the area of the cross-section of flow, and Fr is the Froude number.

The diverted flow rate through the bottom intake is given by

$$Q_d = \int_0^L \frac{dQ}{dx}\,dx, \tag{2}$$

where Q_d is the diverted discharge, and L is the horizontal length of the intake. Generally, the increase of the diverted discharge per unit width of the bottom rack is given by [28,30]:

$$\frac{dq}{dx} = C_d \omega \sqrt{2g\,Y}, \tag{3}$$

where C_d is the discharge coefficient, Y is the suitable value of the effective hydraulic head, dq is the discharge per unit width diverted along with a piece of the grid (dx), and ω is the ratio of the opening area to the total area. The discharge coefficient depends on the geometric properties of the intake structure, such as its length, slope, and orientation; Hydraulic properties such as depth, Froude number and approaching flowrate; and the bottom rack properties (form, size, spacing) [28]. Moreover, the values assumed by C_d are strictly linked to the definition of the effective hydraulic head in Eq. (3).

Bottom racks have several types according to the classification of the opening geometry. These types include longitudinal bars, transversal bars, and perforated screens, among others [9]. In practice, the definition of Y in Eq. (3) depends on the hydraulic performance of each kind of trash rack. For example, when the direction of the flow through a rack opening is nearly straight, as in the case of a rack composed of parallel bars, energy loss is negligible and the effective head on the rack is approximately equal to the specified energy [31,32]. By contrast, when the opening of a rack has an appreciable angle with the streamlines, as in the case of a rack composed of a perforated screen, energy loss through the rack is not negligible and Y is assumed to be equal to the flow depth [31]. Hence, different approaches have been proposed in the literature for evaluating C_d and Y. Therefore, the definitions of Y and C_d, as well as the validation range of the formulas, should be considered carefully to evaluate the diverted discharge in bottom racks.

Energy loss through the porous medium is clearly not negligible. As indicated in Table 2, different relationships have been proposed in the literature for evaluating Q_d in porous bottoms. These formulas are categorized into four types based on the fundamental assumptions used in them. In these relationships, H_1 is the total head of the upstream flow, α

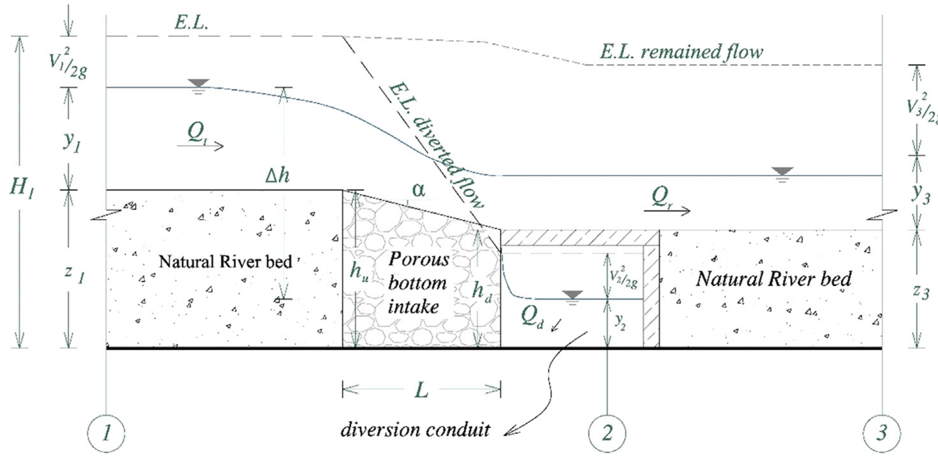

Fig. 1. Definition plot of porous bottom intake.

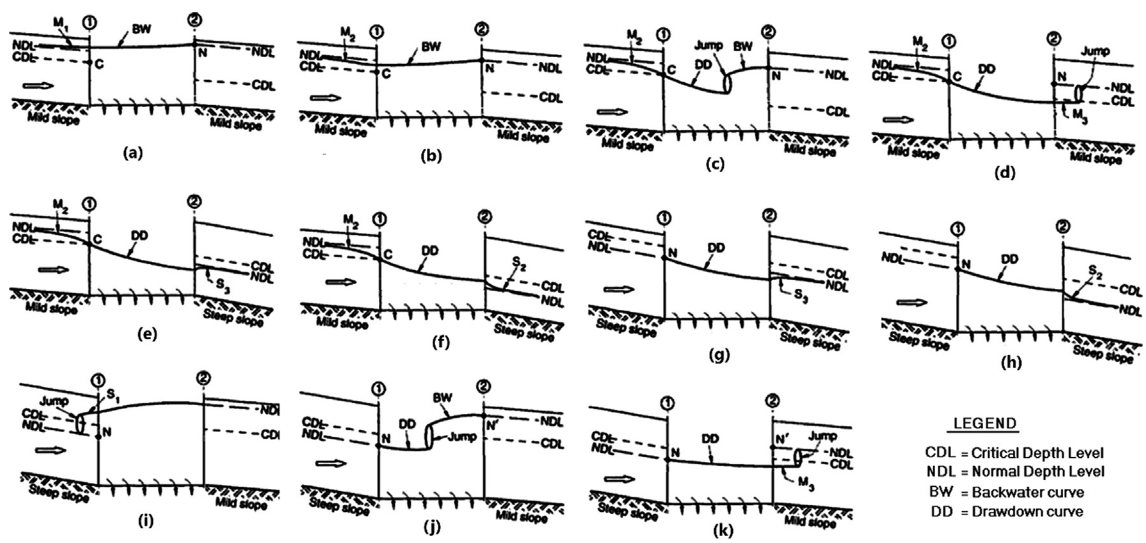

Fig. 2. Types of possible profiles in porous bottom intake.

is the angle between the top surface of the intake and the horizontal direction, z_1 is the upstream elevation of the river bed, y_1 and y_2 are the depths of the upstream flow of the intake and at the diversion conduit, respectively (Fig. 1), S_p is the surface slope of the intake, n is the porosity of the porous medium that fills the intake, W is the intake width, C_d is the discharge coefficient, d_{50} is the mean grain size of the porous medium, Re is the Reynolds number, R_{50} is the ratio of the grain size in the porous medium to the sediment materials at 50% passing, Θ is the dimensionless shear stress (the Shields factor), and σ is the specific deposit. A review of these formulas suggests that the following should be considered to improve previous equations:

1. In the equations of Table 2, $WLn/\cos\alpha$ is the area of the void space that infiltrates water at the top surface of the intake. $Q = \mathbf{V}.\ \mathbf{A}$, hence, the latter part of these equations evaluates the actual velocity of water in the porous medium [33]. The discharge is equal to the

Table 2
Summary of relationships proposed in the literature to estimate the flow discharge through a porous bottom intake.

Equation type	Q_d	C_d	Reference
A	$C_d\frac{WL}{\cos\alpha}n\sqrt{2g(y_1+z_1-y_2)}$	$\propto \frac{\mathrm{Fr}_1^{1.092}\Theta^{0.968}\mathrm{Re}^{0.572}\sigma^{0.269}}{i^{3.157}R_{50}^{0.284}(Sp+y_1/L)^{0.074}}$*	[19]
B	$C_d\frac{WL}{\cos\alpha}n\sqrt{2g(y_1-y_2)}$	$\propto \frac{\mathrm{Fr}_1^{0.739}(y_1/d_{50})^{0.509}}{n^{8.518}(S_p+y_1/L)^{0.363}}$	[33]
B	$C_d\frac{WL}{\cos\alpha}n\sqrt{2g(y_1-y_2)}$	$\propto \frac{\mathrm{Fr}_1^{0.5}\Theta^{0.7}\mathrm{Re}^{0.45}\sigma^{0.261}(Sp+y_1/L)}{i^{2.8}R_{50}^{0.356}}$*	[34]
C	$C_d\frac{WL}{\cos\alpha}n\sqrt{2gH_1}$	$\propto \frac{\mathrm{Fr}_1^{0.664}(y_1/d_{50})^{0.440}}{n^{7.877}(S_p+y_1/L)^{0.332}}$	[35]
D	$C_d\frac{WL}{\cos\alpha}n\sqrt{2g(y_1+z_1)}$	$\propto \frac{\mathrm{Fr}_1^{0.447}(y_1/d_{50})^{0.719}}{n^{9.565}(S_p+y_1/L)^{0.219}}$ *If* $\mathrm{Fr}_1<1$	[35]
D	$C_d\frac{WL}{\cos\alpha}n\sqrt{2g(y_1+z_1)}$	$\propto \frac{\mathrm{Fr}_1^{0.932}(y_1/d_{50})^{0.523}}{n^{8.872}(S_p+y_1/L)^{0.490}}$ *If* $\mathrm{Fr}_1>1$	[35]

* The relationship was proposed to evaluate Q_d in sediment flow.

inner product of velocity and the area vectors. The velocity of flows drained from the surface of the porous bottom is along the vertical direction. Thus, using the horizontal image of the void area $A = WLn$ is better than using that of the inclined area in the proposed equations.

2. The Bernoulli equation is used for estimating velocity in the aforementioned equations. The downstream flow depth of the diversion conduit is ignored in types C and D equations. A further assumption is that the effect of the upstream velocity head is negligible in all types of equations except type C. Furthermore, the total head loss between the main and diverted flows is equal to the difference between the elevation of the upstream and diversion channels in type B equations and negligible in other types. Our observations show that these hypotheses do not corroborate in practice. However, the errors resulting from these assumptions are considered to be compensated by the discharge coefficient [19,33].
3. Obviously, the values assumed by C_d are strictly related to the formula used to estimate Q_d. However, the circumstances of flow diversion in porous bottom are not consistent with the above assumptions. As a result, the relationships of Table 2, contradict several analytical foundations. For example, C_d is directly related to the upstream Froude number (Fr_1) in all relationships, although this variable should clearly be inversely related. Similarly, it is predicted to have a direct relationship between C_d and porosity (n). Nevertheless, the formulas of Table 2 have an inverse relationship between C_d and n.

3. Materials and methods

Based on previous descriptions, a new experimental setup was developed and many experiments were performed to investigate other parameters such as the uniformity coefficient (C_u) and the downstream height of the intake (h_d). This section is devoted to the steps and methods for conducting the experiments.

3.1. Dimensional analysis

The complicated behavior of the flow in porous bottom leads us to use a physical model for studying the hydraulic performance of this type of intakes. The experimental data are used in multivariate regression by an open source program to propose a formula for prediction of diverted discharge. For this purpose, the first step is to determine the independent variables through dimensional analysis. To obtain a generalized formula for predicting the flow rate, all effective parameters should be considered. The physical law that governs the outflow along a porous bottom can be written as follows:

$$q_d = \phi\,(L,\, n,\, y_1,\, g,\, V_1,\, \alpha,\, d_{50},\, h_d,\, C_u,\, S_0,\, \mu,\, \rho), \tag{4}$$

where V_1 is the upstream flow velocity, q_d is the diverted discharge per unit width of the intake, $\mu$is the dynamic viscosity and $\rho$is the density of fluid. All other notations have been defined previously. Thirteen variables and three fundamental quantities are found in Eq. (4), thus, we can extract ten dimensionless parameters as follows:

$$\frac{q_d}{L\,\sqrt{g\,y_1}} = \phi\left(n,\, \frac{y_1}{L},\, \frac{V_1}{\sqrt{gy_1}},\, \alpha,\, \frac{d_{50}}{L},\, \frac{h_d}{L},\, C_u,\, S_0,\, \frac{\rho V_1 y_1}{\mu}\right), \tag{5}$$

where $V_1/\sqrt{gy_1}$ is the upstream Froude number (Fr_1) and $\rho V_1 y_1/\mu$ is the upstream Reynolds number (Re_1). It should be noted that due to the large dimensions of experimental setup and the flow depth (at least 30 mm for the approaching flow), surface tension is negligible. Therefore, the Weber number does not have significant effect on the diversion flow rate (2).

If the selected aggregates are as coarse as possible for obtaining a turbulent flow through the porous medium, then the flow at the top surface of the porous bottom is similar to the flow through the orifices. In this regard, the velocity of the flow through the surface voids of the porous bottoms is assumed to be dependent on the pressure head. Therefore, the hydraulic performance of the porous bottoms is similar to that of bottom racks. Subsequently, Eq. (3) can be used to evaluate the diverted discharge in porous bottoms by using a proper value for the hydraulic head (Y). $y\cos^2\alpha$ is the pressure head at the bed of the channels with heavy slope, thus it can be used as a suitable value for the hydraulic head (Y) in Eq. (3). Furthermore, the void ratio (ω) is equal to the porosity (n) in porous bottoms. As such, Eq. (3) can be rewritten as

$$\frac{dq}{dx} = C_d n \sqrt{2g\, y\cos^2\alpha}\,, \tag{6}$$

for porous bottom intakes. The total diverted discharge through the unit width of a porous bottom is given by:

$$q_d = \int_0^L C_d n \sqrt{2g\, y\cos^2\alpha}\; dx. \tag{7}$$

By assuming that C_d and y are constant, the total discharge diverted by a porous bottom is given by:

$$q_d = C_d n L \sqrt{2g\, y_1 \cos^2\alpha}\,. \tag{8}$$

Substituting q_d from this relationship into Eq. (5) results in

$$C_d n \sqrt{2\cos^2\alpha} \;= \phi\left(n,\, \frac{y_1}{L},\, Fr_1,\, \alpha,\, \frac{d_{50}}{L},\, \frac{h_d}{L},\, C_u,\, S_0,\, Re_1\right). \tag{9}$$

Eq. (9) can be rearranged as follows:

$$C_d = \Phi\left(\frac{y_1}{L},\, Fr_1,\, \frac{d_{50}}{L},\, \frac{h_d}{L},\, C_u,\, S_0,\, Re_1\right). \tag{10}$$

The variables y_1 and Fr_1 obviously depend on the channel slope (S_0). Thus, the S_0 variable has no independent effect on the discharge coefficient, as shown in previous studies [33]. Moreover, due to the limitation on the number of experiments, the experiments are designed at a constant channel slope ($S_0 = 1\%$); So, Eq. (10) becomes

$$C_d = \Phi\left(\frac{y_1}{L},\, Fr_1,\, \frac{d_{50}}{L},\, \frac{h_d}{L},\, C_u,\, Re_1\right). \tag{11}$$

To evaluate the effect of intake properties on C_d, a series of experiments are performed for different intake slopes, namely, 0, 10, and 20%, and various intake lengths i.e. 20, 40, and 60 cm. Furthermore, three types of grain size distribution are used as the porous medium to estimate the effects of C_u and d_{50}. The first grain size (P_D) is the largest ($d_{50} = 19\,mm$), which leads to an almost uniform grain size distribution ($C_u = 1.222$). The other aggregate (P_R) includes the finest grain size with uniform distribution and the last (P_M) has the medium grain size with the largest C_u (Table 3).

Each set of measurements is performed for at least six total discharges ($3 \sim 60\,lit/s$). Additionally, the backwater effect is investigated by adjustment the flow depth in three conditions. Finally, 416 runs are conducted in the laboratory. In each run, several parameters are measured including total, diverted, and remaining discharges, depth and velocity of water at different points, and the piezometric head of porous medium at the bottom of intake.

Table 3
The characteristics of porous bottoms' material in experiments.

Gravel type	d_{max} (mm)	d_{min} (mm)	d_{50} (mm)	γ_d (gr/cm^3)	Cu (d_{60}/d_{10})	n ($\forall_V/\forall_t$)
P_D	25	16	19	1.5	1.222	0.445
P_R	12.5	8	9.5	1.54	1.217	0.428
P_M	25	8	14.25	1.6	1.829	0.402

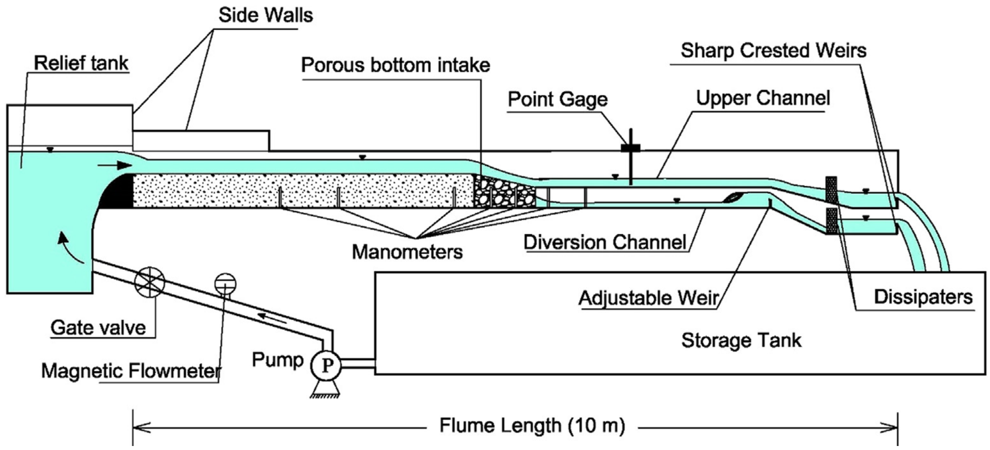

Fig. 3. Longitudinal section of the experimental setup.

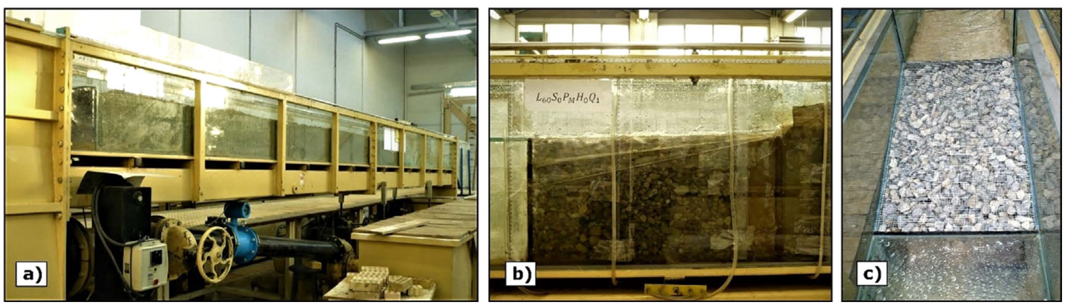

Fig. 4. Experimental setup (a) Setup overview, (b) A view of the porous bottom and (c) The porous bottom and upstream channel.

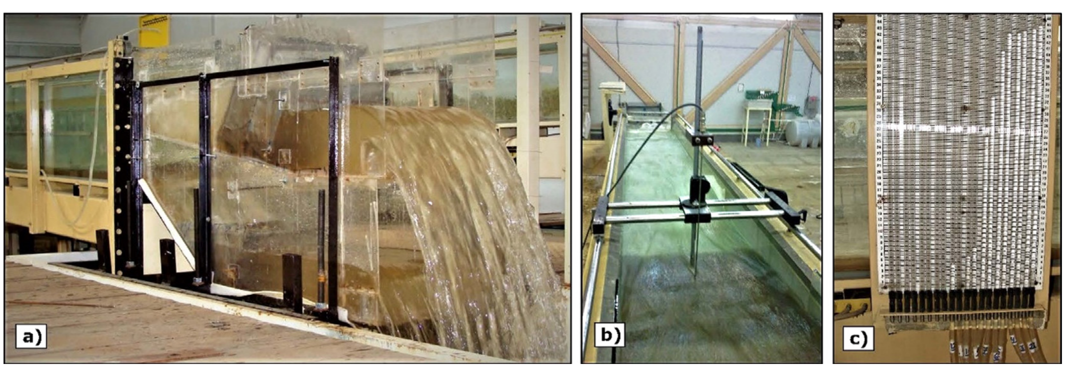

Fig. 5. Supplementary equipment of flume (a) Sharp-crested weirs for measuring remained and diverted discharge, (b) Point gauge and velocimeter and (c) Manometer systems.

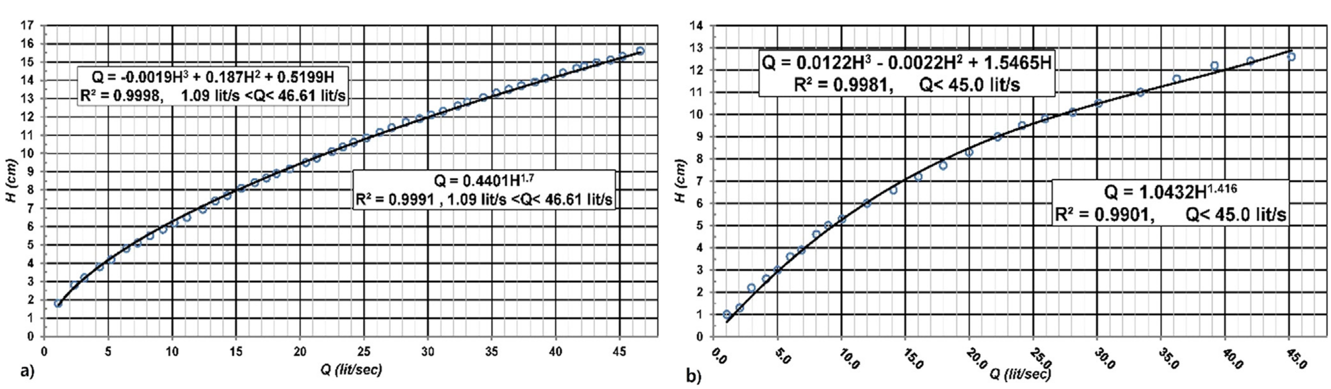

Fig. 6. Calibration formulas for sharp-crested weirs at (a) Upper channel and (b) lower channel.

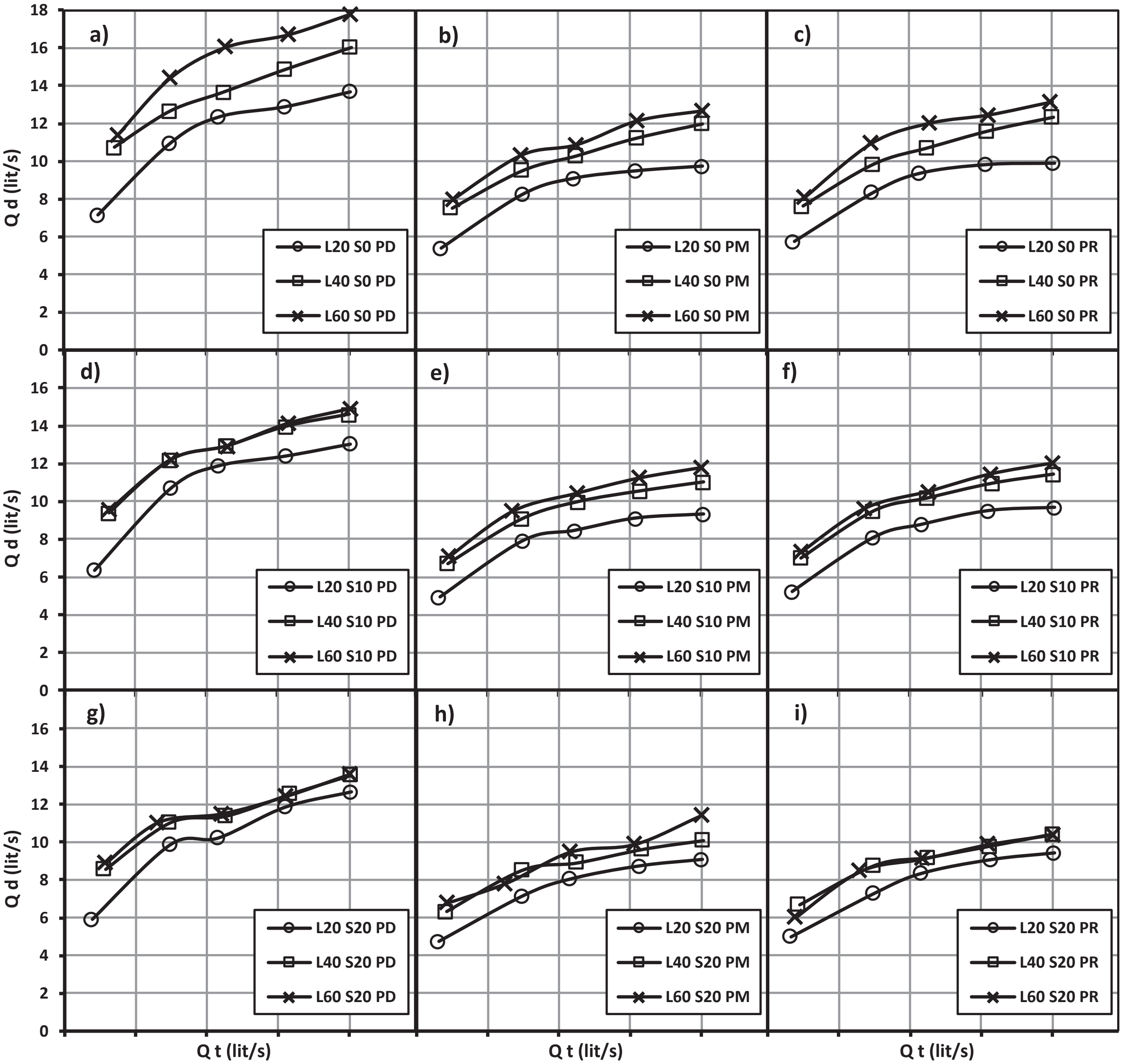

Fig. 7. The variation of diverted discharge due to the different length of intake.

3.2. Experimental setup

The experiments are conducted in a 0.40 m wide and 10 m long rectangular channel (Fig. 3). The flume is equipped with a magnetic flow meter for measuring the total discharge with an accuracy of ± 1%. The depth and velocity of the flow are measured by a point gage and a propeller, respectively. In addition, the intake is built at a 5 m distance from the entrance of the channel to obtain a fully developed flow.

The intake consists of two metal frames placed on the upstream and downstream faces of the intake, which is filled with arbitrary granular materials. The upstream domain of the intake has a constant height. Two inclined sidewalls are used to obtain the surface slope of the intake. For each experiment, the downstream and sidewalls are made separately, according to the different lengths and slopes of the intakes. Furthermore, the upper face of the intake is covered with a wire net (Fig. 4) to prevent the movement of granular materials.

The channel is made as a two-storey flume immediately at the downstream of the intake. The upper and lower channels are used to convey the remained and diverted discharges, respectively. Furthermore, the discharges are measured by rectangular sharp-crested weirs at the end of each stream (Fig. 5(a)). Both weirs are calibrated by the magnetic flowmeter and the discharge relations are extracted (Fig. 6). The flow depth is measured by the point gage and manometers at the upper and lower channels (Fig. 5(b)). Furthermore, the manometers are used to determine the piezometric head at the bottom surface of the intake to establish the authenticity of simulating porous bottoms as bottom racks (Fig. 5(c)).

4. Experimental results

In this section, we present the results of our experiments and discuss them. Hence, by comparing the results, we examine the effect of different parameters on the amount of diversion rate in porous bottoms. The results of this section should be carefully used in the mathematical models generated to simulate the behavior of this type of intakes.

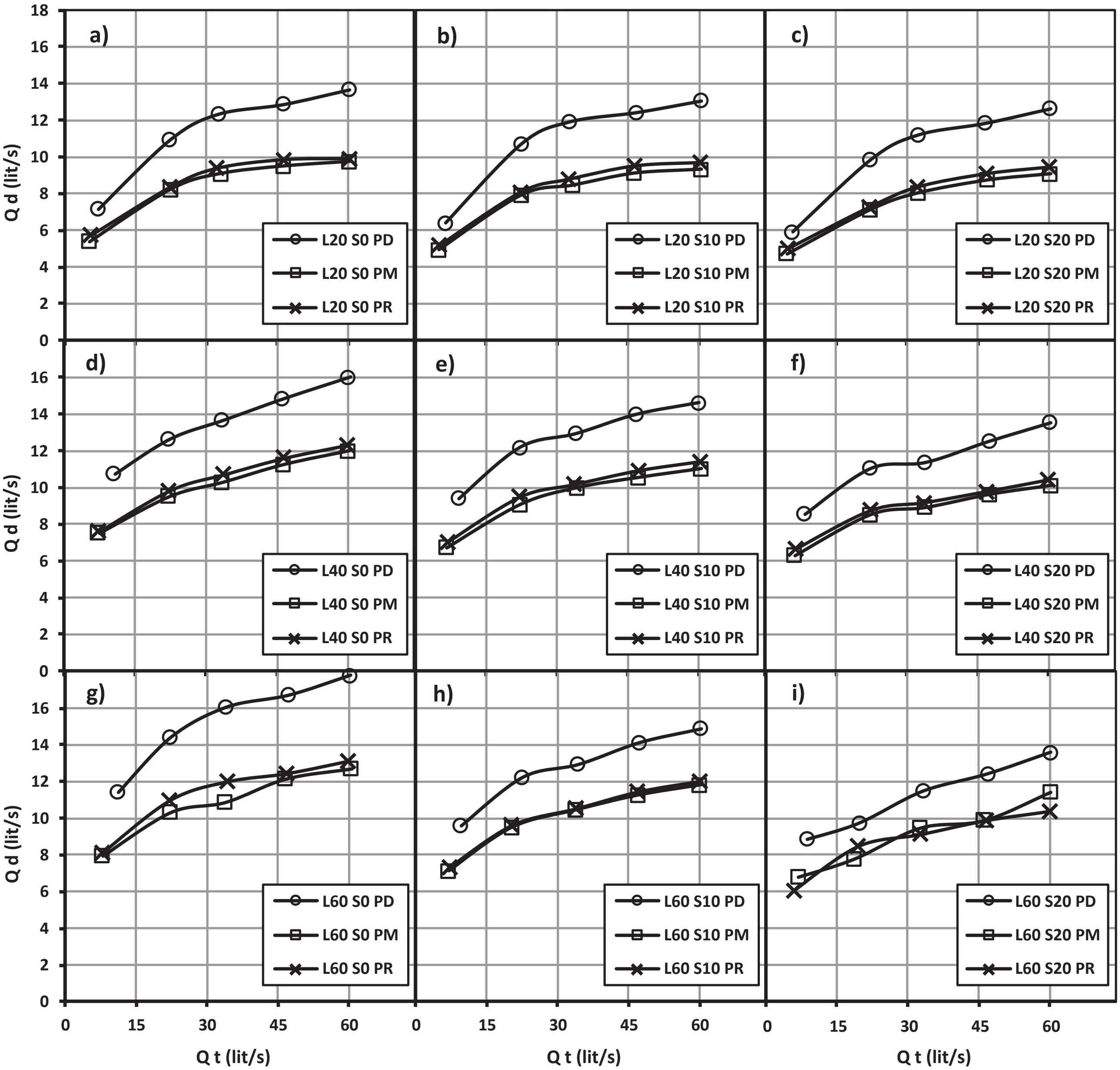

Fig. 8. The variation of diverted discharge due to the different granular material.

4.1. Porous bottoms performance without backwater effect

The effective parameters of the hydraulic performance of the porous bottoms are classified into three categories: the geometric properties of the intake, the grain size distribution of the porous material, and the hydraulic properties of the main flow. The first two categories can be selected by the designers, but the last one depends on the river.

The effects of various parameters on the diverted discharge have been investigated based on the experimental results. In Fig. 7, the diverted discharge (Q_d) is plotted versus the total discharge (Q_t) for different length of intake (L). It is obvious that when L is increased, the diverted discharge is also increased. This behavior is expected because the surface area of intake has a direct relationship with L. However, this effect is limited by other parameters. In other words, we will eventually reach a situation where, as L increases, the diverted discharge will no longer change. This length is named as the maximum effective length of porous bottom intake. A comparison between Fig. 7(d) and (g) shows that the diversion rate is approximately constant for S_P=10% and 20% in P_D material when the length of intake is increased from 40 cm to 60 cm. A similar tendency is observed for $P_M$and P_R materials in S_P = 20% (Fig. 7(h and i). So, the maximum effective length of porous bottom intake depends on certain parameters such as porous medium properties and surface slope.

Fig. 8 shows the variation of Q_d due to different granular materials. By comparing the diverted discharge in coarse and fine aggregates (P_D&P_R), in which the uniformity coefficient is approximately constant, the direct relationship between d_{50} and Q_d becomes clear. In addition, a comparison between fine and mixed aggregates shows that the diversion rate is more in P_R aggregates despite the larger d_{50} in P_M. Thus, C_u is inversely related to Q_d. Theoretically, the diverted discharge depends directly on the porosity and conductivity of the porous medium. Assuming that the compact ratio is constant, then these parameters are related directly to the mean grain size (d_{50}) and inversely to the grain size uniformity coefficient (C_u). Therefore, the observed effects of porous medium properties are in good agreement with the theoretical predictions.

The pressure head at the surface of porous bottoms is obviously related to the diversion flow rate. Therefore, increasing the depth and

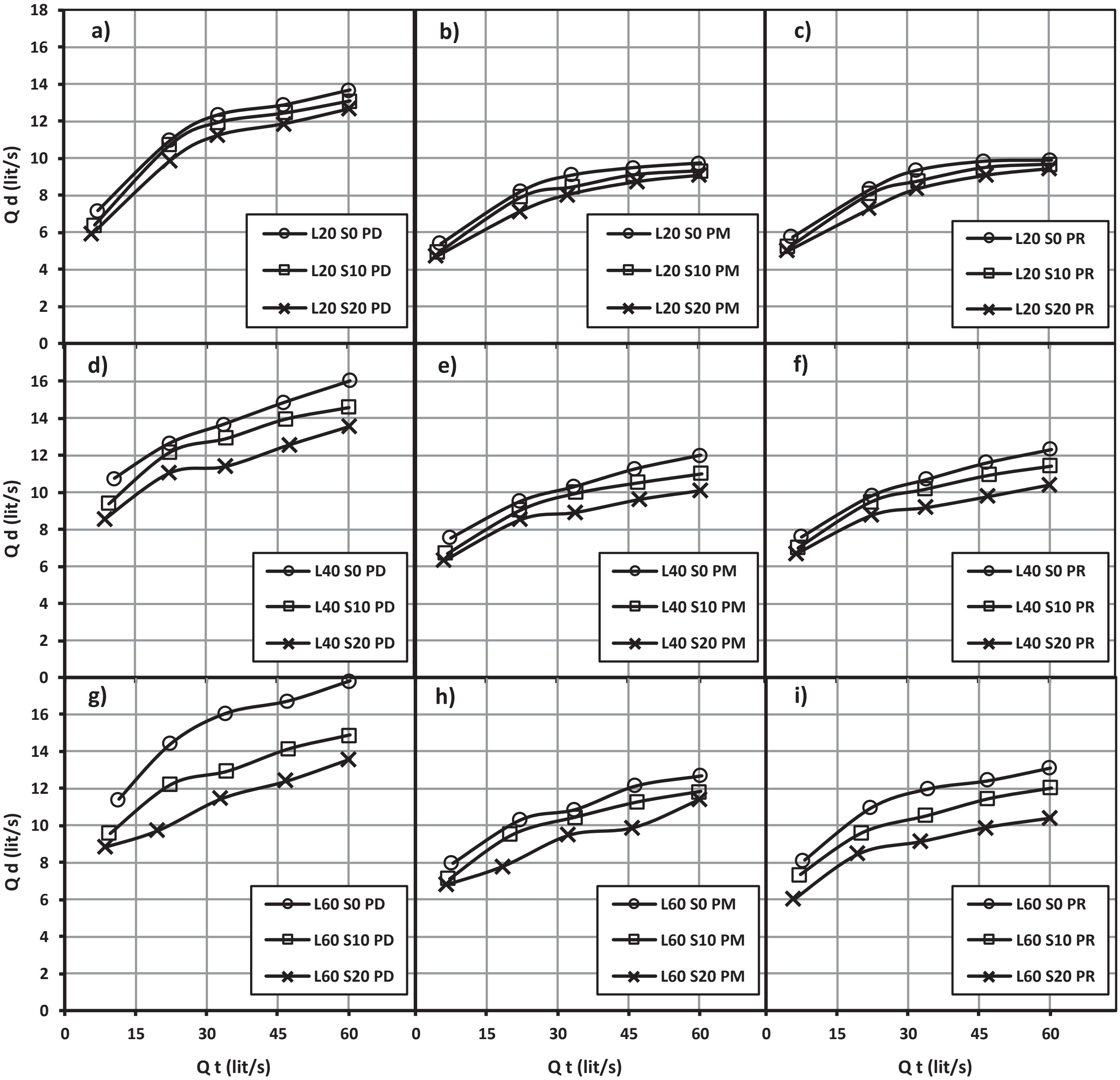

Fig. 9. The variation of diverted discharge due to the different intake slope.

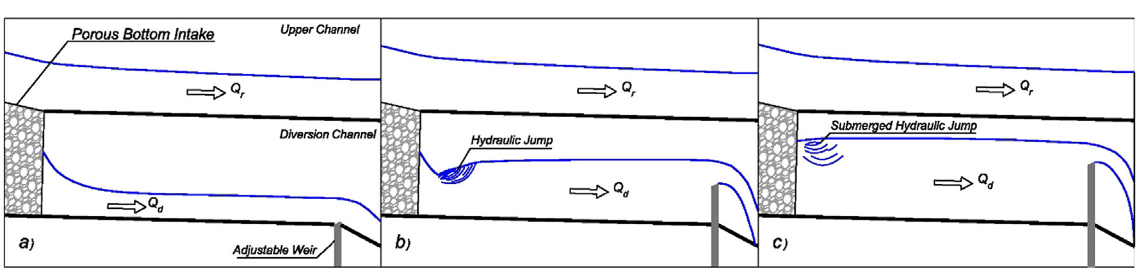

Fig. 10. The flow at diversion conduit (a) Supercritical flow, (b) The hydraulic jump behind the intake and (c) The submerged hydraulic jump.

curvature of the flow lines are considered as additive and regression parameters, respectively. Fig. 9 shows the effect of intake slope for different lengths and materials of porous bottoms. In each series of experiments, the depth of flow depends directly on the total discharge. Therefore, diverted discharges are expected to have a direct relationship with the total discharges. In addition, Fig. 9(g) and (i) show that diverted discharges for steeper slopes at inputs with $L = 60$ cm are reduced. Similar performance is observed for L = 40 cm and L = 20 cm. As a result of the increased the curvature of the flow line, the larger S_P will discharge the smaller diversion.

Eventually, the magnitude of the Froude number (Fr) represents the resistance of the flow to change its direction. Thus, increasing *Fr* leads to a decrease in the deflected current. The above relationships must be carefully considered in any mathematical equation proposed to

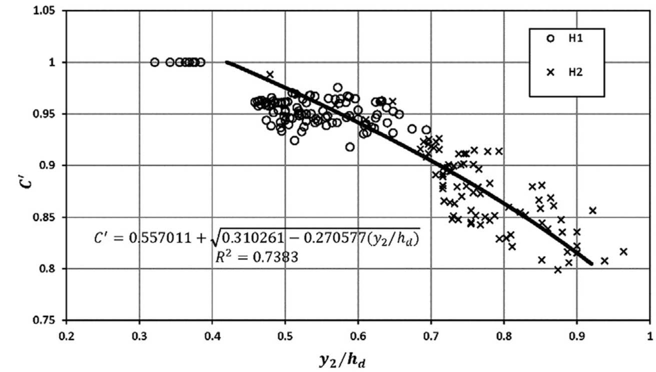

Fig. 11. The backwater effect on the hydraulic performance of porous bottoms.

evaluate the diversion discharge.

4.2. Experimental results in backwater effect

The effect of backwater flow in the diversion conduit can affect the overall performance of the bottom intakes. In our experimental setup, we can adjust the flow depth in the diversion channel by an adjustable sharp-crested weir (Fig. 3). The weir is adjusted in three levels to investigate the backwater effect on the diversion discharge. The flow in the diversion conduit is supercritical at the first level of the weir ($H0$ condition, Fig. 10(a)). At the second level, the backwater causes a hydraulic jump immediately behind the downstream face of the intake ($H1$ condition, Fig. 10(b)). Finally, at the last level, the hydraulic jump is completely submerged because of the backwater effect ($H2$ condition, Fig. 10(c)).

Table 4
The range of dimensionless parameters on experimental data.

	Fr_1	y_1/L	h_d/L	C_u	d_{50}/L	Re_1	n
Minimum	1.00	0.014	0.316	1.217	0.016	2880	0.402
Maximum	2.00	0.557	1.550	1.829	0.095	451,542	0.445

The results of the experiments related to the backwater effect are presented in Fig. 11. In this figure, C' is the ratio of the diverted discharge in $H1$ and $H2$ to $H0$ conditions. Therefore, the decrease in diverted discharge resulting from backwater submergence can be obtained from

$$0.42 < (y_2/h_d) \leqslant 0.9, Q_d' = C' Q_d, \quad (12)$$

where Q_d' is the diverted discharge when the backwater effect is considered. As shown in Fig. 11, if $y_2/h_d \leqslant 0.42$, then tailwater depth does not affect the performance of porous bottoms. The decrease in discharge resulting from the backwater effect can be evaluated by

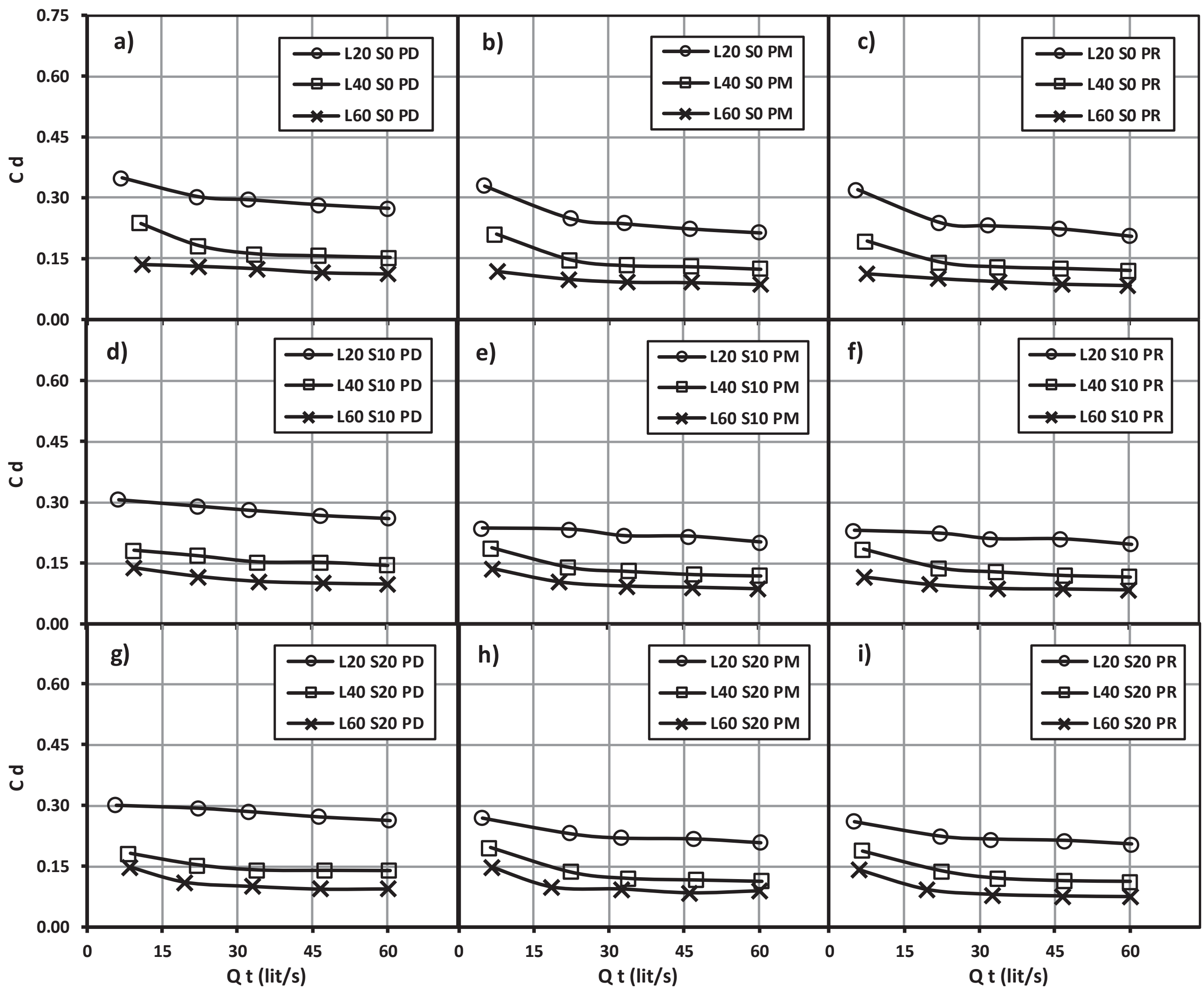

Fig. 12. Variation of C_d as a function of discharge Q_t.

Table 5
The output of multivariate regression on experimental data.

Parameter estimation				
Parameter	Estimate	Std. Error	95% Confidence Interval	
			Lower Bound	Upper Bound
c1	2.014	1.349	−0.655	4.683
c2	−0.073	0.094	−0.259	0.113
c3	0.000	0.080	−0.159	0.159
c4	0.400	0.066	0.269	0.530
c5	−0.220	0.036	−0.291	−0.149
c6	0.315	0.024	0.268	0.362
c7	−0.120	0.053	−0.225	−0.016

ANOVA[a]			
Source	Sum of Squares	df	Mean Squares
Regression	4.330	7	0.619
Residual	0.024	128	0.000
Uncorrected Total	4.355	135	
Corrected Total	0.604	134	

Dependent variable: C_D.
[a] R squared = 0.960.

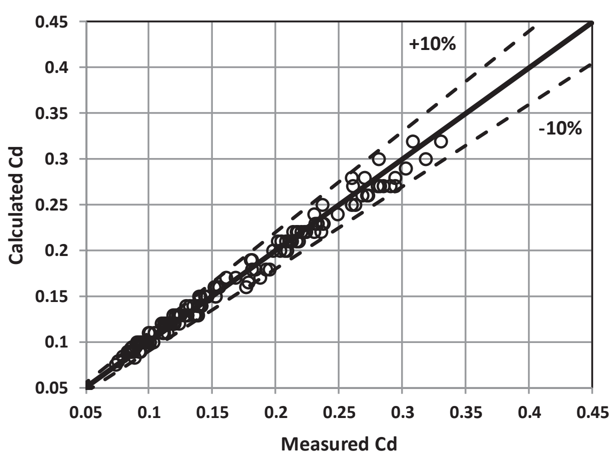

Fig. 13. Correlation between calculated and measured C_d.

estimating C' from the following equation:

$$C' = 0.557011 + \sqrt{0.310261 - 0.270577(y_2/h_d)},\ :0.42 < (y_2/h_d) \leqslant 0.9. \tag{13}$$

5. Estimation of discharge coefficient

In previous sections, we introduced a general formulation for evaluating the diversion discharge (Eq. (8)). The effect of all simplifying assumptions is compensated by the discharge coefficient (C_d). Also, we suggested a new function for assessment of C_d by dimensional analysis in Eq. (11). In this section, we use the experimental measurements of this research to accomplish the multivariate regression for estimation of C_d.

Fig. 12 presents the variation of C_d for different lengths, materials and surface slopes of porous bottoms. It is obvious that in each series of the experiments, the depth, Froude number and Reynolds number of flows, directly depend on the total discharge. As shown in Fig. 12, C_d has inverse relationship with Q_t and L. Also by comparing the results for different materials of the porous bottom, it is found that C_d has a direct and inverse relationship with d_{50} andC_u, respectively.

The best nonlinear fit to our measured data is found to be

$$C_d = 2.014 Fr_1^{-0.073}\left(\frac{y_1}{L}\right)^{0.000}\left(\frac{h_d}{L}\right)^{0.400} C_u^{-0.220}\left(\frac{d_{50}}{L}\right)^{0.315} Re_1^{-0.120}. \tag{14}$$

This equation is only valid for $y_2/h_d \leqslant 0.42$. Other limitations of using Eq. (14) are presented in table 4. The coefficient of determination of Eq. (14) is $R^2 = 0.960$. Table 5 shows the output results of the multivariate regression for this equation.

Equation (14) is in accordance with the predicted behavior of the discharge coefficient discussed earlier in Fig. 12. Also, the power of the term y_1/L becomes zero, so the discharge coefficient is independent of this parameter.

The correlation between the calculated and measured C_d values is presented in Fig. 13. As shown in this figure, all the calculated C_d values are within the range of ± 10% from the measured C_d. Moreover, the combination of Eqs. (14) and (8) satisfied all the aforementioned theoretical expectations.

6. Conclusions

In this study, we focused on hydraulics of porous bottom intake in non-sediment flow. To achieve this aim, the independent variables were recognized through dimensional analysis. Moreover, an experimental setup was constructed and numerous experiments were conducted under different hydraulic conditions. Finally, the mathematical equations were introduced to evaluate the diversion rate and discharge coefficient.

This study illustrated that the diversion discharge of porous bottoms directly depends on the horizontal length of intake, the flow depth at the beginning of intake, as well as porosity and mean grain size of the granular medium. Furthermore, the Froude number of the main flow, the uniformity coefficient of grain size distribution, and the top surface slope of intake have an inverse relationship with the diversion rate.

The results of this study are consistent with the theoretical basis of intake behavior. Therefore, the proposed formulas can be generalized to new conditions. Such general application is the main advantage of this work over previous studies. Furthermore, we suggest using the proposed structures in mountainous rivers, which lack fine sediments, particularly in small hydropower plants.

Declaration of Competing Interest

The authors declare that they have no known competing financial interests or personal relationships that could have appeared to influence the work reported in this paper.

Acknowledgements

The authors would like to thank the editors and anonymous reviewers for their comments that help improve the manuscript.

References

[1] M. Bouvard, Mobile Barrages and Intakes on Sediment Transporting Rivers, Balkema, Rotterdam, Netherlands, 1992, p. 300.
[2] K. Bina, H. Saghi, Experimental study of discharge coefficient and trapping ratio in mesh-panel bottom rack for sediment and non-sediment flow and supercritical approaching conditions, Exp. Therm Fluid Sci. 88 (2017) 171–186.
[3] M. Andaroodi, A. Schleiss, Standardization of Civil Engineering Works of Small High-head Hydropower Plants and Development of an Optimization Tool, EPFL-LCH, 2006.
[4] S. Brunella, W.H. Hager, H.-E. Minor, Hydraulics of bottom rack intake, J. Hydraul. Eng. 129 (1) (2003) 2–10.
[5] H. Lauterjung, G. Schmidt, Planning of Water intake structures for irrigation or hydropower. A Publication of GTZ-Postharvest Project in: Deutsche Gesellschaft für Technische Zusammenarbeit (GTZ) GmbH. 1989.
[6] G. Noseda, Operation and design of bottom intake racks, in: 6th International Association of Hydraulic Research Congress; 1955; La Haye.
[7] H. Drobir, V. Kienberger, N. Krouzecky, The Wetted Rack Length of The Tyrolean Weir. IAHR-28th Congress; Graz, Austria,1999.
[8] F. Xiang, L.M. Kavvas, Z. Chen, H. Bandeh, N. Ohara, S. Kim, et al., Experimental

study of debris capture efficiency of trash racks, J. Hydro-environ. Res. 3 (3) (2009) 138–147.
[9] J.M. Carrillo, L.G. Castillo, J.T. García, Á. Sordo-Ward, Considerations for the design of bottom intake systems, J. Hydroinf. 20 (1) (2017) 232–245.
[10] Z. Suzhen, Laboratory investigation of bottom-grated intake structure, J. Hydraulic Eng. 9 (1983) 64.
[11] J.J. Strong, R. Ott, Intake screens for small hydro plants, Hydro Rev. 7 (1988) 66–69.
[12] P. Dušička, M. Ozábal, Water intake structures on small hydropower plants, Eleltroenergetika 4 (2) (2011).
[13] J. Garcia, L. Castillo, P. Haro, J. Carrillo, Occlusion in bottom intakes with circular bars by flow with gravel-sized sediment. An experimental study, Water 10 (11) (2018) 1699.
[14] R. Itsukushima, S. Ikematsu, M. Nakano, M. Takagi, Y. Shimatani, Optimal structure of grated bottom intakes designed for small hydroelectric power generation, J. Renew. Sustain. Energy 8 (3) (2016) 034501.
[15] D. Huber, BEDUIN Project. Trondheim, Norway: Norwegian University of Science and Technology (N.T.N.U), 2005.
[16] S. Lund, Inntak til Småkraftverk, Norwegian University of Science and Technology (N.T.N.U), Trondheim, Norway, 2005.
[17] A.H.A. Dehwah, T.M. Missimer, Subsurface intake systems: green choice for improving feed water quality at SWRO desalination plants, Jeddah Saudi Arabia, Water Res. 88 (2016) 216–224.
[18] M.F. Maghrebi, New System of Bottom Intake with Porous Media, Water Resources Management, Khorasan Razavi Province, Iran, 2009.
[19] B. Naghavi, M.F. Maghrebi, Experimental study of sediment flow discharge in new system of bottom intakes with porous media, Transp. Porous Media 85 (2010) 867–884.
[20] R. Mansouri, A.N. Ziaei, K. Esmaili, H, Ansari (Eds.), Study on a new river subsurface water harvesting method, in: 18th IAHR-APD, Jeju, Korea.
[21] F. Garot, De Watervang met liggend rooster, Ing Ned Indie. 7 (1939).
[22] G. De Marchi, Profili longitudinali della superficie libera delle correnti permanenti lineari con portata progressivamente crescente e progressivamente decrescente entro canali a sezione costante, 1947.
[23] M. Bouvard, Debit d'une grille par en dessous (Discharge passing through a bottom grid), Houille Blanche 3 (1953) 290–291.
[24] J. Orth, E. Chardonnet, G. Meynardi, Etude de Grilles pour Prises d'eau du Type. en-dessous, La Houille Blanche 9 (6) (1954) 343–351.
[25] S. Kumar, Z. Ahmad, U.C. Kothyari, M.K. Mittal, Discharge characteristics of a trench weir, Flow Meas. Instrum. 21 (2) (2010) 80–87.
[26] M.J. Carrillo, T.J. García, G.L. Castillo, Experimental and numerical modelling of bottom intake racks with circular bars, Water 10 (5) (2018).
[27] S.N. Chan, C.K.C. Wong, J.H.W. Lee, Hydraulics of air–water flow in a supercritical bottom rack intake, J. Hydro-environ. Res. 21 (2018) 60–75.
[28] M. Righetti, S. Lanzoni, Experimental study of the flow field over bottom intake racks, J. Hydraul. Eng. 134 (1) (2008) 15–22.
[29] S.C. Jain, Open-channel flow, Wiley, New York; Chichester, 2000.
[30] A.A. Kamanbedast, M. Shafai Bejestan, Effects of slope and area opening on the discharge ratio in bottom intake structures, J. Appl. Sci. 8 (14) (2008) 2631–2635.
[31] R.H. Frénch, Open-channel Hydraulics, McGraw-Hill, 1985.
[32] G.K. White , A. CJ, W. RCA (Eds.), On the Design of Bottom Intakes for Diverting Stream Flows, in: Proc Of Institution of Civil Engineers, London, England, 1972.
[33] F. Kooroshvahid, K. Esmaili, B. Naghavi, Experimental study on hydraulic characteristics of bottom intake with granular porous media, Spec. Top. Rev. Porous Media – Int. J. 2 (4) (2011) 301–311.
[34] B. Naghavi, M.F. Maghrebi, K. Esmaili, S. Khodashenas, F. Kooroshvahid, On the comparison of the diverted discharges in a bottom intake with porous media in clear water and sediment flow, J Water Soil 23 (3) (2009) 122–135.
[35] F. Kooroshvahid, K. Esmaili, M.F. Maghrebi, A. Alizadeh, B. Naghavi, Flow discharge in bottom intakes with porous media, J. Water Soil 24 (2) (2010) 347–358.